

# Accurate Spectral Efficiency Analysis for Non Orthogonal Multiple Access

Pongsatorn Sedtheetorn, Tatcha Chulajata

*Department of Electrical Engineering, Faculty of Engineering, Mahidol University  
25/25 Phuttamonthon 4 Road, Salaya, Nakornpathom, Thailand  
pongsatorn.sed@mahidol.ac.th, tatcha.chu@mahidol.ac.th*

**Abstract**— This paper presents theoretical analysis on non-orthogonal multiple access (NOMA) for both downlink and uplink communications. Based on accurate evaluation, we propose closed-form expressions of NOMA downlink and uplink spectral efficiency. In terms of channel modelling, we map the channel conditions with Nakagami and Rayleigh models in which both line-of-sight and non-line-of-sight are included. For uplink transmission, we extend our work to the case of random active users. The random nature is matched to appropriate probability models. These make our presented expressions very comprehensive and benefit us to study the impacts of channel conditions, random number of users, and other key system parameters on the NOMA spectral efficiency.

**Keyword**— Non orthogonal multiple access, 5G mobile communication, uplink, downlink, spectral efficiency

## I. INTRODUCTION

Recently, the growth of mobile communication is rapidly rising. In the next generation, the entries to mobile networks are not only from human but also from machines. This makes the demand go even greater. It is important noting that radio access technology plays an important role. The current radio access technology, orthogonal frequency multiple access (OFDMA), might not be the best option due to the issues of spectral efficiency and power utilization [1].

As mentioned above, the new radio access technology, namely non-orthogonal multiple access (NOMA), has been introduced [2]-[7]. Based on NOMA, every users share the whole spectrum and each individual is multiplexed to one another via power domain. On the receiver end, the known successive interference cancellation (SIC) method [8] is employed to extract the desired signal from stronger interferences by cancelling (subtracting) them with

superposition coding. From the results therein [5], NOMA provides 30% more throughput than the traditional orthogonal multiple access (OMA), which is OFDMA.

In terms of research challenges, there are many aspects to concern. The area on spectral efficiency analysis gains a huge interest, e.g. [3]-[7]. For instance, [4]-[5] focus on the spectral efficiency estimation in which all parameters are however set constantly. The work in [6] is on the analysis of outage probability which is directly related to the spectral efficiency. Others are on the throughput maximization problems such as [3], [7].

Nevertheless, the analysis in the literature still leaves some tasks unfinished. Especially some random-nature parameters such as channel gains and the number of active users are fixed or conditioned owing to the sake of simplicity.

In contrast to the literature, here we present accurate original analysis on NOMA spectral efficiency inclusively on both downlink and uplink transmissions. Furthermore, the impact of random channel gains is mathematically mapped by the famous Nakagami model in which line-of-sight and non-line-of-sight scenarios are taken into account. Also, on the uplink, we model the random number of active users with corresponding probability processes. This makes our work far more practical and outstandingly distinguished from the others.

This paper is organized as follows. Section II illustrates the system model that includes all assumptions and parameters used in this paper. Section III shows the original analysis on NOMA downlink and uplink spectral efficiency. Sequentially, the exact closed forms are presented. Section IV demonstrates the numerical and simulation results. Section V draws the conclusion of this work.

## II. SYSTEM MODEL

In this section, the scenario of the future radio access technology, namely NOMA, is explained in terms of both downlink and uplink transmissions. Moreover, all assumptions, key system parameters and performance are defined. Since the transmissions are on wireless channels, the magnitudes of channel gains at a receiver end are inevitably random. Here, the models of channel gains are also classified to cover all possible characteristics of signal propagation.

---

Manuscript received February 25, 2016. This work is a follow-up of the invited journal to the accepted out-standing conference paper of the 18th International Conference on Advanced Communication Technology (ICACT2016).

P. Sedtheetorn is with the Department of Electrical Engineering, Faculty of Engineering, Mahidol University, Nakornpathom, 73170, Thailand (corresponding author, phone: 66-2889-2225 ext. 6501-3; fax: 66-2889-2225 ext. 6529; e-mail: pongsatorn.sed@mahidol.ac.th).

T. Chulajata is with the Department of Electrical Engineering, Faculty of Engineering, Mahidol University, Nakornpathom, 73170, Thailand (e-mail: tatcha.chu@mahidol.ac.th).

**A. Downlink Communication**

Figure 1 describes the scenario of NOMA downlink communication. The base station, called eNodeB, serves multiple user equipments (UEs). It is known that NOMA multiplexes individuals in power domain, each of which uses the SIC technique and is able to perfectly decode the signals from the weakest ones.

To demonstrate this, Figure 2 shows the spectrum allocation of NOMA and OMA (e.g. OFDMA). In the figure, the downlink powers of individual UEs are assigned unequally based on their distances from the serving eNodeB. Without the loss of generality, UE1 is assumed to be the closet one with the lowest dedicated power, while UE2, UE3, ..., UE *N* stay further with more dedicated powers. This technique is called rank adaption [2] in which  $P_{UE1} < P_{UE2} < \dots < P_{UEN}$  and  $P_{UE1} + P_{UE2} + \dots + P_{UEN} = P$ . Next, the eNodeB sends every UE a downlink signal with the total power *P*. Then, each UE uses its SIC receiver to extract the desired signal. For example, UE1 uses SIC receiver to filter out stronger signals of UE2, UE3, ..., UE *N*.

In this work, the power spectral of zero-mean additive Gaussian white noise (AWGN) is assumed as  $N_0$ . The power gains of UE1, UE2,...UE *N* can be defined by  $|h_1|^2, |h_2|^2, \dots, |h_N|^2$ . Recall the technique rank adaptation, we have

$$|h_1|^2 / N_{0,1} > |h_2|^2 / N_{0,2} > \dots > |h_N|^2 / N_{0,N} \quad (1)$$

where  $|h_n|^2 / N_{0,n}$  is defined as signal to noise ratio (SNR) of UE *n*.

Obviously, the signal power at the receiver end of UE *n* is

$$S_n = |h_n|^2 P + N_{0,n} \quad (2)$$

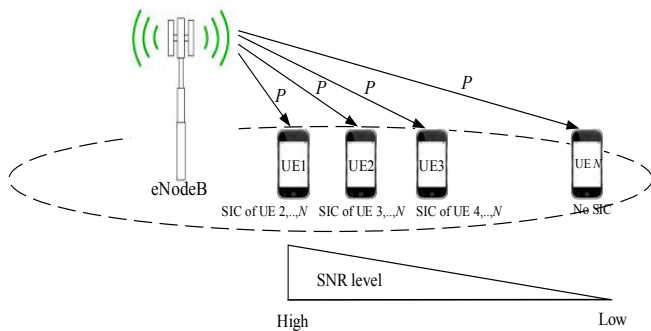


Fig. 1. Downlink NOMA with SIC technique

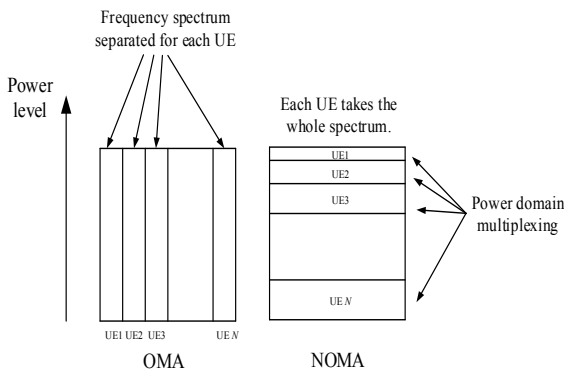


Fig. 2. NOMA vs OMA (OFDMA)

Based on SIC process, UE *n*,  $n \in \{1,2,\dots,N\}$ , can remove the inter-user interference from UE *n*+1 whose SNR level is smaller,  $|h_{n+1}|^2 / N_{0,n+1} < |h_n|^2 / N_{0,n}$ . On the assumption of band-limited waveforms in AWGN channel, the spectral efficiency of UE *n* can be declared as [4]

$$C_n = \log_2 \left( 1 + \frac{P_n |h_n|^2}{\sum_{i=1}^{n-1} P_i |h_i|^2 + N_{0,n}} \right) \quad (3)$$

which is in bps/Hz and for  $n \in \{1,2,\dots,N\}$ . Now, we can define the signal-to-interference-plus-noise ratio (SINR) =  $P_n |h_n|^2 / \sum_{i=1}^{n-1} P_i |h_i|^2 + N_{0,n}$ .

**B. Uplink Communication**

Consider uplink transmissions in Figure 3. Every UE is able to transmit their information through multiple subcarriers, which is called multi-carrier transmissions. Note that the multi-carrier technique, so called carrier aggregation, is preferably used in the future mobile communication in order to increase the overall throughput.

Based on NOMA technique, UEs are allowed to share the same resource simultaneously both in the aspects of frequency spectrum and time. Therefore, the receiver at the eNodeB is required to operate multi-user detection (MUD) in order to distinguish signals of individual UEs. One of favorite MUD techniques is SIC in which the desired signal is recovered from the subtraction (cancellation) of interferences.

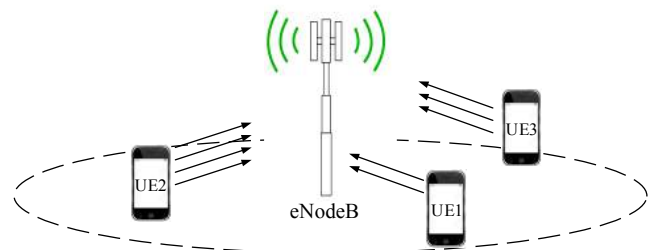


Fig. 3. Uplink multi-carrier NOMA

To this point, the signal received at the eNodeB can be expressed as

$$S_n = \sum_{i=1}^N \sum_{l=1}^L P_{i,l} |h_{i,l}|^2 + N_0 \quad (4)$$

where *L* is the maximum number of subcarriers of individual UE.  $P_{i,l}$  and  $|h_{i,l}|^2$  are the power and the gain of the signal from UE *i* on the particular subcarrier *l*.

Similarly, the uplink spectral efficiency of UE *n* is [3]

$$C_n = \sum_{l=1}^L \log_2 \left( 1 + \frac{P_{n,l} |h_{n,l}|^2}{\sum_{i=1, i \neq n}^N P_{i,l} |h_{i,l}|^2 + N_0} \right) \quad (5)$$

where the term  $\sum_{i=1, i \neq n}^N P_{i,l} |h_{i,l}|^2$  acts as the interferences of the desired signal  $P_{n,l} |h_{n,l}|^2$  on subcarrier *l*. Likewise, the uplink SINR =  $P_{n,l} |h_{n,l}|^2 / \sum_{i=1, i \neq n}^N P_{i,l} |h_{i,l}|^2 + N_0$ .

### C. Channel Modelling

Owing to the fact that the power gains are random throughout wireless channel, appropriate probability models are required to complete the analysis. In this work, we apply two famous probability models, namely Rayleigh fading and Nakagami fading.

It is known that Nakagami fading is a comprehensive model that covers both line-of-sight (LOS) and non-line-of-sight (NLOS) scenarios via the index  $m$  as shown in Table 1 and the mathematical model is illustrated in Section II-C2.

**Table I.**  
NAKAGAMI FADING INDEX [9]

Nakagami fading index $m$	Propagation environments
1	NLOS (urban areas)
2-4	obstructed areas
5	suburban areas
6	open plain

In terms of Rayleigh fading, this model is considered as a special case in which a pair of transmitter and receiver stay NLOS. Rayleigh model is regularly used in research work to analyze the extreme case of signal propagation. Furthermore, its mathematical model is expressed by a negative exponential random variable which is quite simple in comparison to the gamma-distributed Nakagami fading.

#### 1) The special case: Rayleigh fading

In the case of NLOS, there is no dominant signal. The received signals scatter from all around directions. A channel gain (voltage gain),  $h(t)$ , is depicted in terms of imaginary number  $h(t) = h_i(t) + j h_j(t)$  in which each component is a Gaussian random variable due to the center limit theory.

Then, the magnitude,  $|h(t)|$ , stands for Rayleigh process and its square,  $|h(t)|^2$ , becomes a power gain representing a unit-mean negative exponential random variable with probability density function

$$f_{|h(t)|^2}(z) = e^{-z}. \quad (6)$$

When apply power gains to (3) either or (5), the spectral efficiency becomes a function of multi random variable.

In the literature, the spectral efficiency can be determined by simulating all possible power gain values and then averaging out the result. In some past work e.g. [4]-[5], the gains remain fixed for simplicity.

Alternatively, the average of spectral efficiency can be calculated directly via the multiple integrations of the interferences' density functions. This consumes huge computation time and yields complexity.

In this work, we propose efficient method to accurately calculate the average spectral efficiency of NOMA. Thanks to the properties of exponential distribution, we can use these properties to solve this mathematical difficulty (see Section III).

#### 2) The general case: Nakagami fading

Assume that the signal (channel) gain  $h_n$ ; models Nakagami fading. The corresponding power gain  $|h_n|^2$  becomes a

unit-mean gamma random variable with probability density function [10]

$$f_{|h_n|^2}(z) = \frac{z^{m-1}}{\Gamma(m)} m^m e^{-mz} \quad (7)$$

where  $0.5 \leq m < \infty$  is Nakagami fading index and  $\Gamma(m) = (m-1)!$  is the gamma function. When  $m=1$ , the probability density function is exponentially distributed which models Rayleigh fading (NLOS fading).

At this point, it is seen that Nakagami fading model covers both NLOS (Rayleigh) and LOS cases. Moreover, the dominant signal (LOS signal) turns to be stronger when  $m$  goes larger.

### III. NOMA SPECTRAL EFFICIENCY ANALYSIS

This section illustrates the analysis of NOMA spectral efficiency both for downlink and uplink. The analysis starts from the special case, Rayleigh fading, to the general case, Nakagami fading, which has more mathematical complexity. As a result, we propose new accurate closed-form expressions of NOMA uplink and downlink spectral efficiency. Furthermore, for uplink, we extend our work to consider the case when the number of active UEs is random.

#### A. Downlink Analysis

The analysis can be categorized to Rayleigh and Nakagami fading as follows;

##### 1) Rayleigh fading environment

On the condition of Rayleigh fading, the power gains are exponentially distributed random variables. Consider the system model in Section II-A. Now the average spectral efficiency, assumed successful decoding and no error propagation, of UE  $n$  can be presented as

$$C_{n,avg} = E[\log_2(1 + \text{SINR})] = \int_0^{\infty} \log_2(1+z) f_{\text{SINR}}(z) dz. \quad (8)$$

We can see that there is some complexity on the integration of the probability density function of SINR,  $f_{\text{SINR}}(z)$ . To tackle such the problem, a new efficient method to calculate the spectral efficiency is introduced as below.

Rearrange (8) with the change of logarithmic base, then we have

$$C_{n,avg} = \log_2 e \int_0^{\infty} P(\text{SINR} > z) \frac{dz}{1+z} \quad (9)$$

where  $f_{\text{SINR}}(z) dz = dP(\text{SINR} > z)$ . Here we use the property of an exponential random variable  $X$ ,  $P(X > \mu) = e^{-\mu}$ , when  $\mu$  is a constant.

Owing to the fact that  $|h_n|^2$  is also exponentially distributed, therefore

$$P(\text{SINR} > z) = e^{-\frac{z}{P_n} \left( \sum_{i=1}^{n-1} P_i |h_i|^2 + N_{0,n} \right)}. \quad (10)$$

To compute the average spectral efficiency, one needs to find the average of cumulative function  $P(\text{SINR} > z)$ . Fortunately, the average value of the cumulative function can be determined by calculating the moment generating function (MGF) of  $|h_n|^2$ . It is known that the MGF of any exponential

random variable  $X$  is  $E[e^{-\beta X}] = 1/(1 + \beta)$  for a constant  $\beta$ . Then,

$$E\left[e^{-\frac{z}{P_n} \left(\sum_{i=1}^{n-1} P_i |h_i|^2 + N_{0,n}\right)}\right] = e^{-zN_{0,n}/P_n} \prod_{i=1}^{n-1} \left(\frac{1}{1 + (P_i/P_n)z}\right). \quad (11)$$

Replace the MGF derived in (11) into (9). As a result, the closed-form expression of the downlink spectral efficiency of NOMA is

$$C_{n,avg} = \log_2 e \int_0^\infty \frac{e^{-zN_{0,n}/P_n}}{1+z} \prod_{i=1}^{n-1} \left(\frac{1}{1 + (P_i/P_n)z}\right) dz. \quad (12)$$

Hint that this closed form presents the exact average of the spectral efficiency without any loss of generality in Rayleigh fading environment. Moreover, the closed form can be used in OMA case by simply adding the orthogonal multiplexing factor  $\alpha$ .

Denote  $\alpha_1, \alpha_2, \dots, \alpha_N$  by the orthogonal multiplexing factors of UE1, UE2, ..., UE  $N$  and  $\sum_{i=1}^N \alpha_i = 1$ . The power allocation for each UE is identical to one another,  $P_1 = P_2 = \dots = P_N = P$ , as a result the spectral efficiency of UE  $n$  is

$$C_{n,OMA} = \alpha_n \log_2 e \int_0^\infty \frac{e^{-zN_{0,n}/P_n}}{(1+z)^n} dz. \quad (13)$$

### 2) Nakagami fading environment

Recall (8) with the change of logarithm. Then, we have

$$C_{n,avg} = \log_2 e \int_0^\infty \ln(1+z) f_{\text{SINR}}(z) dz \quad (14)$$

Now we cannot use the method as in Section III-1A because the density function of SINR is the combination of multiple gamma random variables. Fortunately, we sort this problem by the following *Lemma 1*.

*Lemma 1:* Let  $u$  be a unit-mean gamma random variable with a probability density function  $f(u) = \frac{u^{m-1}}{\Gamma(m)} m^m e^{-mu}$  and  $v$  be any non-negative random variable and independent from  $u$ .

Let  $z = u/v$  where  $u = |h_n|^2$ ,  $v = \frac{1}{P_n |h_n|^2} \left(\sum_{i=1}^{n-1} P_i |h_i|^2 + N_{0,n}\right)$ , and

$$E[\ln(1+z)|v] = \int_0^\infty \frac{1}{z} \left[1 - \frac{1}{(1+z)^m}\right] \text{MGF}(mz) dz. \quad (15)$$

*Proof:* we know that  $\ln(1+z) = z {}_2F_1(1; 1; 2; -z)$  where  ${}_2F_1(a; b; c; z)$  is a Gauss hyper geometric function [11]. Next we get

$$\begin{aligned} & \frac{1}{(m-1)!} \frac{d^m}{dz^m} z^{m-1} \ln(1+z) \\ &= \frac{1}{(m-1)!} \frac{d^m}{dz^m} z^m {}_2F_1(1; 1; 2; -z) \\ &= m {}_2F_1(1+m; 1; 2; -z) \\ &= m \int_0^\infty (1+tz)^{-(m+1)} dt = \frac{1}{z} - \frac{1}{z(1+z)^m}. \end{aligned} \quad (16)$$

Also, the MGF can be solved in a simpler form,

$$\text{MGF}(mz) = e^{-zmN_{0,n}/P_n} \prod_{i=1}^{n-1} \left(\frac{1}{1 + \frac{P_i}{P_n} z}\right). \quad (17)$$

Replace MGF( $mz$ ) in (15) and (14) respectively. As a result, the average spectral efficiency of downlink NOMA in Nakagami fading is

$$C_{n,avg} = \log_2 e \int_0^\infty \frac{e^{-zmN_{0,n}/P_n}}{z} \left[1 - \frac{1}{(1+z)^m}\right] \prod_{i=1}^{n-1} \left(\frac{1}{1 + \frac{P_i}{P_n} z}\right) dz. \quad (18)$$

### B. Uplink Analysis

Likewise, the closed-form spectral efficiency of uplink can be derived by the same procedures as those of downlink. However, another issue on the uplink is the randomness of active UEs. In practice, the number of active UEs (during voice either or data transmission) is unknown to the eNodeB. Here we investigate the effect of random number of UEs and extend our closed forms to include this case.

#### 1) Fixed number of users

Recall (5) and the procedure to achieve (15). We derive the closed form of uplink NOMA spectral efficiency in Rayleigh fading as

$$C_{n,avg} = \log_2 e \sum_{l=1}^L \left\{ \int_0^\infty \frac{e^{-zN_{0,l}/P_{n,l}}}{1+z} \prod_{i=1, i \neq n}^N \left(\frac{1}{1 + (P_{i,l}/P_{n,l})z}\right) dz \right\}. \quad (19)$$

Similarly, recall the same procedure to accomplish (18). We have the uplink spectral efficiency in Nakagami fading as

$$\begin{aligned} C_{n,avg} &= \log_2 e \sum_{l=1}^L \left\{ \int_0^\infty \frac{e^{-zmN_{0,l}/P_{n,l}}}{z} \left[1 - \frac{1}{(1+z)^m}\right] \right. \\ & \left. \prod_{i=1, i \neq n}^N \left(\frac{1}{1 + (P_{i,l}/P_{n,l})z}\right)^{-1} dz \right\}. \end{aligned} \quad (20)$$

Let all UEs be active simultaneously, then the total spectral efficiency is as  $C_{tot} = NC_n$ . In practice, the number of active UEs is however random and distributed from 0, 1, 2, ...,  $N$ . In the next section, we therefore sort this problem and put the effect of random UEs in the proposed expressions.

#### 2) Random number of users

In this paper, we can model the randomness of active UEs by Poisson and binomial distributions. The Poisson model seems reasonable when the total number of both active and inactive UEs is unknown at the eNodeB. Then the amount of active UEs is estimated by statistically average value. For binomial model, the total number of UEs is determined and the number of active UEs is defined by a certain on-off (active-inactive) probability. These assumptions (Poisson and binomial) could be available in practice.

##### a) Poisson distribution

In terms of Poisson process, the number of active users is approximated by the average value  $\lambda$ . Then, the probability mass function (pmf) can be written as [10]

$$\Pr(N = k) = \frac{\lambda^k}{k!} e^{-\lambda} \quad (21)$$

where  $k$  is the number of active UEs at an instance. Hint that, when the number of interfering UEs is random, we need to recalculate  $C_{n,avg}$ . For example, recall (19) and assume all transmitted uplink powers are identical. Without the loss of generality, the spectral efficiency becomes

$$\mathbb{E} \left[ e^{\frac{-zm}{P_{n,l}} \left( \sum_{i=1, i \neq n}^N P_{i,l} |h_{i,l}|^2 + N_0 \right)} \right] = e^{-\lambda} \left( \frac{1}{1+z} \right)^{N-1}. \quad (22)$$

*Lemma 2:* Let  $V(\cdot)$  be any function and  $Y$  be a Poisson random variable with parameter ( $\lambda$ ). Then, we have

$$\mathbb{E}[V^Y(\cdot)] = e^{-\lambda[V(\cdot)-1]}. \quad (23)$$

*Proof:* Let  $t$  be a constant. The moment generating function of  $Y$  is  $\mathbb{E}[e^{tY}]$ ,

$$\text{MGF}(Y) = \mathbb{E}[e^{tY}] = \sum_{k=0}^{\infty} e^{tk} \frac{\lambda^k}{k!} = e^{-\lambda} \sum_{k=0}^{\infty} \frac{(e^t \lambda)^k}{k!}. \quad (24)$$

We know that the summation of the pmf is equal to 1; i.e.

$\sum_{k=0}^{\infty} e^{-\lambda} \lambda^k / k! = 1$ , then  $\sum_{k=0}^{\infty} \lambda^k / k! = e^{\lambda}$ . Apply this to  $\text{MGF}(Y)$ , thus it becomes

$$\text{MGF}(Y) = e^{-\lambda} e^{e^t \lambda} = e^{\lambda(e^t - 1)}. \quad (25)$$

Replace  $e^t$  with function  $V(\cdot)$ . Finally we have the proof of *Lemma 2*.

Apply *Lemma 2* to (19). Then, we have the spectral efficiency of individual UE. As a result, the total spectral efficiency becomes

$$C_{\text{tot}} = \lambda C_n. \quad (26)$$

Note that we can apply *Lemma 2* to (20) for the spectral efficiency in Nakagami fading as well.

#### b) Binomial distribution

Recall (22). Now  $N$  is binomially distributed. Let us declare *Lemma 3*.

*Lemma 3:* Let  $V(\cdot)$  be any function and  $Y$  be a binomial random variable with parameters ( $N, p$ ). Then, we have

$$\mathbb{E}[V^Y(\cdot)] = [1 - p + pV(\cdot)]^N \quad (27)$$

*Proof:* if  $Y$  is a binomial random variable with parameters ( $N, p$ ). The MGF of  $Y$  is  $\mathbb{E}[e^{tY}]$  in which  $t$  is a constant. Then,

$$\begin{aligned} \mathbb{E}[e^{tY}] &= \sum_{k=0}^N e^{tk} \binom{N}{k} p^k (1-p)^{N-k} \\ &= \sum_{k=0}^N \binom{N}{k} (pe^t)^k (1-p)^{N-k} = [1 - p + pe^t]^N. \end{aligned} \quad (28)$$

Replace  $e^t$  with function  $V(\cdot)$ , thus we yield the same result as in (27).

Apply (27) to (19). The exact average uplink spectral efficiency is

$$C_{n,\text{avg}} = \log_2 e \sum_{l=1}^L \left\{ \int_0^{\infty} \frac{e^{-zN_0/P_{n,l}}}{1+z} \left[ 1 - p + p \left( \frac{1}{1+z} \right) \right]^{N-1} dz \right\}. \quad (29)$$

As a result, the overall spectral efficiency is

$$C_{\text{tot}} = pNC_n \quad (30)$$

where  $pN$  is the average value of a binomial random variable with parameter ( $N, p$ ). Note that the spectral efficiency in the case of Nakagami fading can be derived by the same manner.

## IV. NUMERICAL RESULTS AND DISCUSSIONS

In this section, selected numerical results and simulation results are shown. The results are categorized to uplink and downlink aspects each which represents different scenarios of NOMA spectral efficiency versus key system parameters. Furthermore, we also validate our numerical results,

proposed from our expressions, with the simulation. In terms of simulation results, we apply Monte Carlo simulation in which the random power gains are generated and the spectral efficiency is computed by the original Shannon formula (see equation (3) and (5) for downlink and uplink respectively). Then, we repeat the iterations over 2,000,000 times to make sure the results reliable.

### A. Downlink Communication

Consider a single-cell environment with three UEs, namely UE1, UE2, and UE3, respectively. UE1 is the nearest one to the eNodeB whereas UE2 stays further away from the eNodeB and UE3 is the furthest. Then, the power allocations are  $P_1=1/6$ ,  $P_2=1/3$ ,  $P_3=1/2$  for UE1, UE2, and UE3, respectively. Let  $\text{SNR} = P/N_0$  where  $P = P_1 + P_2 + P_3$ . Assume that the fading index  $m=1$  represents non-line-of-sight propagation which models Rayleigh fading.

In Figure 4, our numerical results, generated from (12), is positively matched to those of the simulation. This validates the accuracy of our proposed expression. In the figure, the expression is used to evaluate the NOMA spectral efficiency of each UE against the SNR in dB. Obviously, the spectral efficiency of UE1 (the nearest one) is higher than others because it has the highest rank adaptation (highest SINR) which supports the principle of NOMA with SIC receivers.

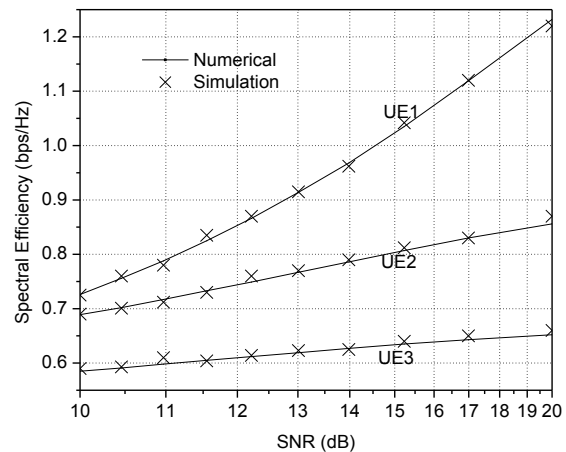


Fig. 4. NOMA spectral efficiency: validation of the proposed expression (numerical result) with the simulation

In addition, we can extend our work to compute the spectral efficiency of OMA (OFDMA) (see equation (13)). From Figure 5, the overall spectral efficiency of NOMA is up to 30% higher than those of OMA which is identical to the results in [5].

Figure 5 demonstrates four different power allocation plans, i.e. A, B, C, and D with various power proportions for individual UEs. Note that the spectral efficiency plotted in this figure is the summed value, i.e.  $C = C_1 + C_2 + C_3$ . It can be seen that the power proportion of far UE should be greater to gain better overall spectral efficiency (plan A). With this allocation plan, the spectral efficiency however rapidly drops when SNR goes lower than 17 dB. Thus, the power allocation plan B seems the most optimal solution in this scenario.

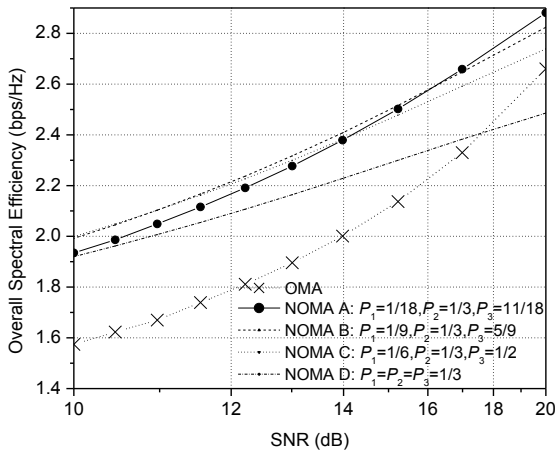


Fig. 5. NOMA spectral efficiency with different power allocation plans (plan A, B, C, and D) versus OMA (OFDMA)

Next, the evaluation of NOMA spectral efficiency in Nakagami fading is taken into account (see equation (18)). Figure 6 illustrates the impact of channel conditions on the spectral efficiency. Here the channel conditions are represented by the integer fading index  $m$ . It is known that, when  $m=1$ , the channel acts as Rayleigh model in which the line-of-sight between transmitters and receivers disappears. Otherwise, when  $m$  is larger, the dominant line-of-sight becomes more obvious and the spectral efficiency increases.

From Figure 6, it is worth saying that the impact of fading index  $m$  on the spectral efficiency is greater than that of SNR. We can observe that, when  $m=1,2$  (highly obstructed channel), the impact of SNR, considered as background noise, is unobvious. On the other hand, when the channel is clear (high  $m$ ), SNR plays a role in the degradation of spectral efficiency.

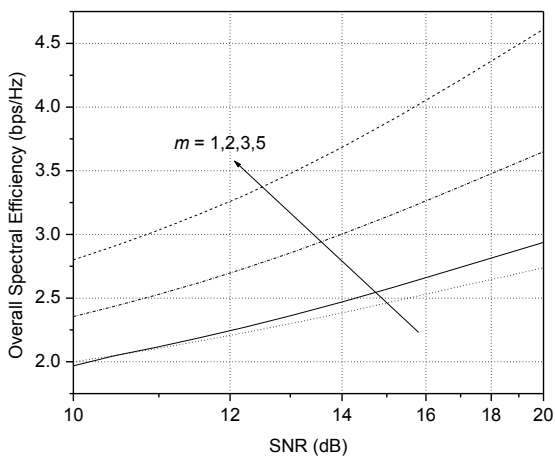


Fig. 6. NOMA spectral efficiency with different fading indices

**B. Uplink Communication**

In this section, we focus on uplink communication. Assume that there are 5 active UEs, each of which occupies 3 subcarriers, in the cell and their power transmissions are in the same level. Hint that signal-to-noise ratio (SNR) is defined as  $SNR = P_{n,i}/N_0$  in decibel (dB).

Figure 7 illustrates the impact of channel conditions on the spectral efficiency. It is known that, when  $m = 1$ , the channel

acts as Rayleigh model in which there is no LOS between the eNodeB and its UEs. On the other hand, when  $m$  is larger, the dominant line-of-sight becomes more obvious and the spectral efficiency increases.

Again, the solid lines, representing numerical results, are matched to the cross symbols of the simulation. This can confirm the validation of our proposed expression in (20).

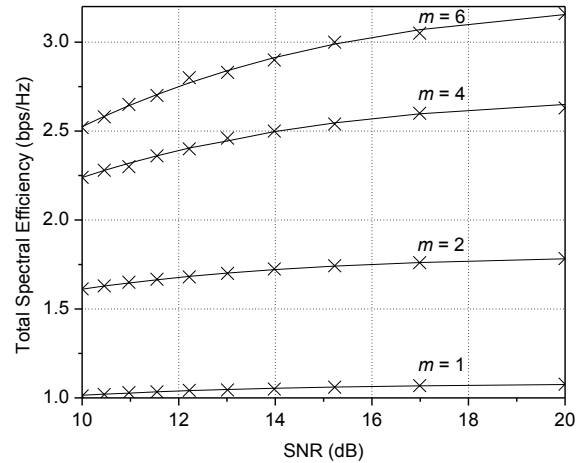


Fig. 7. Total uplink spectral efficiency at different fading index

In Figure 8, we plot the uplink spectral efficiency (equation (26)) versus SNR ( $m=1$ ) in the case that number of active UEs are random and Poisson distributed. Assume that all UEs use 3 subcarriers to convey their information ( $L=3$ ).  $\lambda$  varies from 2, 3, 5 and 10. It is seen that increasing number of active UEs reflects on interferences to one another and the decrease of the spectral efficiency.

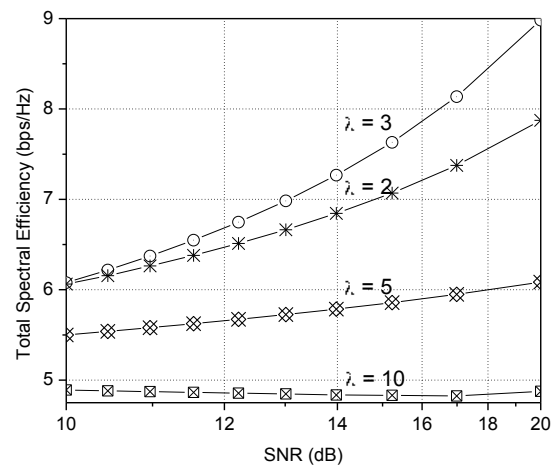


Fig. 8. Total uplink spectral efficiency at varying arrival rate

In Figure 9, the total spectral efficiency versus SNR with varying active probability in (30) is concerned. Here the number of active UEs is binomially distributed. The total number of UEs is  $N=10$ . All UEs use 3 subcarriers to convey their information ( $L=3$ ). In the figure, the active probability ( $p$ ) varies from 0.1, 0.3, 0.5, 0.7, and 0.9.

It is seen that high value of active probability activates UEs to transmit their signals and thus interfere one another. This leads to the drop of the overall spectral efficiency. Moreover, we find that the appropriate value is around 0.3 or

3 active users at an instance which is equal to the optimal Poisson arrival rate ( $\lambda=3$ ) in Figure 8.

To have more demonstration on this issue, let see Figure 10. SNR is set as 10 dB and all UEs use 3 subcarriers to convey their information while the total number of UEs ( $N$ ) varies from 5, 7, 15, and 20. From the figure, we can get the optimal condition when the total number of UEs is around 3.

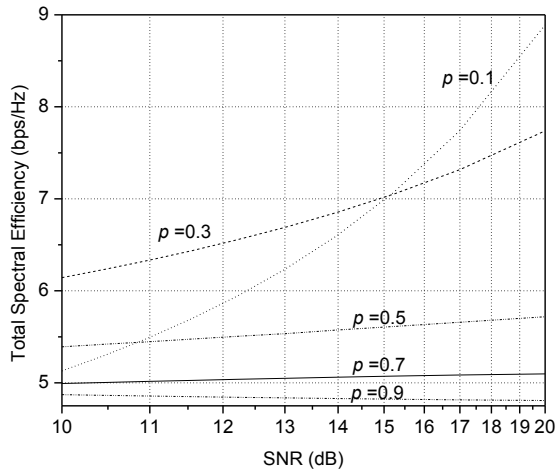


Fig. 9. Total uplink spectral efficiency at different active probabilities

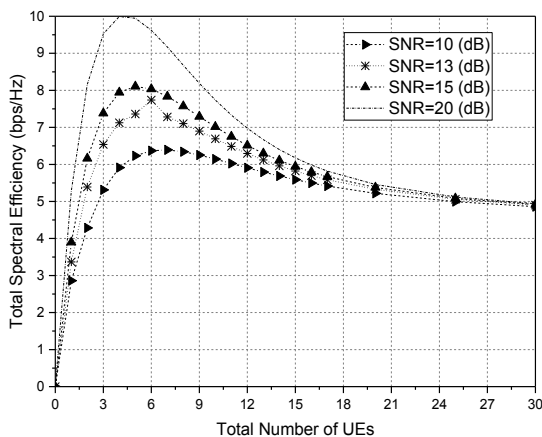


Fig. 10. Total uplink spectral efficiency at different values of SNR

## V. CONCLUSION

This paper has presented original analysis on NOMA spectral efficiency for both downlink and uplink. This has introduced new exact closed forms of NOMA downlink and uplink spectral efficiency. The closed forms also reflect the channel condition via Nakagami fading index. Furthermore, the effect of random users on uplink is taken into account and characterized with different probability models. This benefits us to accurately investigate the impacts of channel conditions, random active users, and key system parameters on the NOMA spectral efficiency.

From the results, we have found that the impact of channel blockage on the spectral efficiency is far more obvious than that of the background noise (represented by SNR). Furthermore, especially on the uplink, the number of active users directly reflects the amount of interferences. When the arrival rate (for Poisson model) or active probability (for binomial) is greater, the overall spectral efficiency decreases.

However, there is an optimal number of active users to achieve the highest spectral efficiency at a certain provided bandwidth. In this paper, the optimal point of binomial distributed model is equal to that of Poisson distributed. This also reasonably confirms and validates our proposed expressions.

## REFERENCES

- [1] Jeffrey G. Andrews *et al.*, "What will 5G be?," *IEEE Journal on Selected Areas in Commun.*, vol. 32, no. 6, pp. 1065-1082, June 2014.
- [2] Docomo 5G white paper, "5G radio access: requirements, concept and technologies," NTT Docomo Inc., 2014.
- [3] Mohammed Al-Imari *et al.*, "Uplink non-orthogonal multiple access for 5G wireless networks," in *IEEE Proceeding of ISWCS*, vol. 1, August 2014, pp. 781-785.
- [4] Yuya Saito *et al.*, "Non-orthogonal multiple access (NOMA) for cellular future radio access," in *IEEE Proceeding of VTC Spring*, vol. 1, June 2013, pp. 1-5.
- [5] Anass Benjebbour *et al.*, "Concept and practical considerations of non-orthogonal multiple access (NOMA) for future radio access," in *IEEE Proceeding of ISPACS*, vol. 1, November 2013, pp. 770-774.
- [6] Zhiqiu Ding *et al.*, "On the performance of non-orthogonal multiple access in 5G systems with randomly deployed users," *IEEE Trans. on Signal Processing Lett.*, vol. 21, no. 12, pp. 1501-1505, December 2014.
- [7] Stelios Timotheou *et al.*, "Fairness for non-orthogonal multiple access in 5G systems," *IEEE Trans. on Signal Processing Lett.*, vol. 22, no. 10, pp. 1647-1651, October 2015.
- [8] Mazen O. Hasna *et al.*, "Performance analysis of mobile cellular systems with successive co-channel interference cancellation," *IEEE Trans. on Wireless Commun.*, vol. 2, issue 1, pp. 29-40, February 2003.
- [9] John G. Proakis *et al.*, *Digital Communications*, 5th edition, Mc-GrawHill, 2008.
- [10] Sheldon M. Ross, *Introduction to probability models*, 7th edition, Harcourt Academic Press, 2000.
- [11] S.M. Abramowitz, *Handbook of mathematical functions with formulas, graphs, and mathematical tables*, U.S. Department of Commerce, 1972.



**Pongsatorn Sedtheetorn** (M'03) received the B.Eng. and M.Eng. degrees from Chulalongkorn University, Thailand, in 1998 and 2001, and the Ph.D. degree from the University of Manchester, United Kingdom, in 2007. He is currently an Associate Professor with the Department of Electrical Engineering, Mahidol University, Thailand. His research interests are in the areas of wireless communications, information theory, as well as enterprise architecture.



**Tatcha Chulajata** (M'97) received the B.Eng. from Kasetsart University, Thailand, in 1992. He received the M.S and the Ph.D. degrees from Wichita State University, USA, in 1996 and 2003, respectively. He is currently a Senior Lecturer with the Department of Electrical Engineering, Mahidol University, Thailand. His research interests are in the areas of wireless communications, communication network, and enterprise architecture.